WATER RESOURCES RESEARCH, VOL. 34, NO. 4, PAGES 855–862, APRIL 1998

On the sensitivity of drainage density to climate change

Glenn E. Moglen

Department of Civil Engineering, University of Maryland, College Park

Elfatih A. B. Eltahir and Rafael L. Bras

Ralph M. Parsons Laboratory, Department of Civil and Environmental Engineering
Massachusetts Institute of Technology, Cambridge

Abstract. Drainage density reflects the signature of climate on the topography and dictates the boundary conditions for surface hydrology. Hence defining the relationship between drainage density and climate is important in assessing the sensitivity of water resources and hydrology to climate change. Here we analyze the equilibrium relationship between drainage density and climate and estimate the relative sensitivity of drainage density to climate change. We conclude that the sign of the resulting change in drainage density depends not only on the direction of the change in climate but also on the prevailing climatic regime.

1. Introduction

The predictions of a global climate change that may result from the evident change in the chemical composition of Earth's atmosphere raise several questions regarding the potential impacts of such change on water resources, agriculture, and ecosystems, three issues with immense importance to society. These valuable resources depend to a significant degree on soil moisture conditions, runoff production, river flow, and in general on the hydrology of continental land masses. The geomorphology of a river basin defines the boundary conditions for these important hydrologic processes. Hence understanding the response of river networks to climate change is an important step in the process of assessing the sensitivity of hydrology and water resources to the same process.

Drainage density, defined as the total length of channels per unit area of the basin, is an important property of a river network. This geomorphic measure reflects the prevailing conditions of climate, soil texture, land use, and tectonics as well as their complex interactions that result in observed landforms. Drainage density is closely linked to several hydrologic processes including infiltration, soil saturation, sheet erosion, overland flow, and their interactions that control the production of runoff and sediment. The drainage density exhibited by a basin is at the heart of the balance between climate, geomorphology, and hydrology.

2. Background

Drainage density defines the extent to which streams dissect a topography. The key feature quantified by drainage density is thus the channel head, or stream source. Considerable debate exists over the precise location of the channel head as determined from digital terrain data or even from field surveys [*Montgomery and Foufoula-Georgiou*, 1993]. Does one consider intermittent or ephemeral streams? Does a hollow with a saturated floor constitute a stream? We refer the reader to the work of *Montgomery and Dietrich* [1988, 1994] for a discussion of this issue. This paper instead employs the shift in dominance from diffusive to fluvial mass transport as a surrogate scale for the channel head source area. This physically corresponds to the scale at which convex hilltops give way to concave valleys. *Smith and Bretherton* [1972] show this is the scale at which valleys will grow and interpret this as channelization.

Paper number 97WR02709.
0043-1397/98/97WR-02709$09.00

The importance of drainage density as a geomorphic and hydrologic characteristic was recognized early by quantitative geomorphologists. *Horton* [1945] used the reciprocal of twice the drainage density to obtain the average length of overland flow. In doing so Horton implicitly related hydrologic response to drainage density. *Schumm* [1956] defined a constant of channel maintenance as the inverse of drainage density.

Gregory and Walling [1968, p. 67] state the following:

> Drainage density is the dynamic manifestation of varying inputs into the drainage basin system and its relation to particular inputs reflects the basin characteristics; it is through drainage density that these characteristics influence the output of water and sediment from the system.

They conclude that streamflow goes as drainage density to a positive power, commonly 2. They warn about consistency of comparisons because of variability in the estimation of drainage density.

Using the Buckingham Pi theorem, *Strahler* [1964] carried out a dimensional analysis and expressed drainage density as a function of three dimensionless terms:

$$D_d = \frac{1}{H} f\left(Q_r K, \frac{Q_r \rho H}{\mu}, \frac{Q_r^2}{gH} \right) \tag{1}$$

where D_d is the drainage density (L^{-1}); H is basin relief (L); $f(\quad)$ is a function; Q_r is runoff intensity ($L^{-1}T^{-1}$); K is an erosion proportionality factor (ratio of erosion intensity to eroding force) with units ($L^{-1}T$); ρ is fluid density (ML^{-3}); μ is dynamic viscosity of the fluid ($ML^{-1}T^{-1}$); and g is the acceleration of gravity (LT^{-2}). He wrote (p. 4.52) that

> In general, low drainage density is favored in regions of highly resistant or highly permeable subsoil material, under dense vegetative cover, and where relief is low. High drainage density is favored in regions of weak or impermeable subsurface materials, sparse vegetation and mountainous relief.

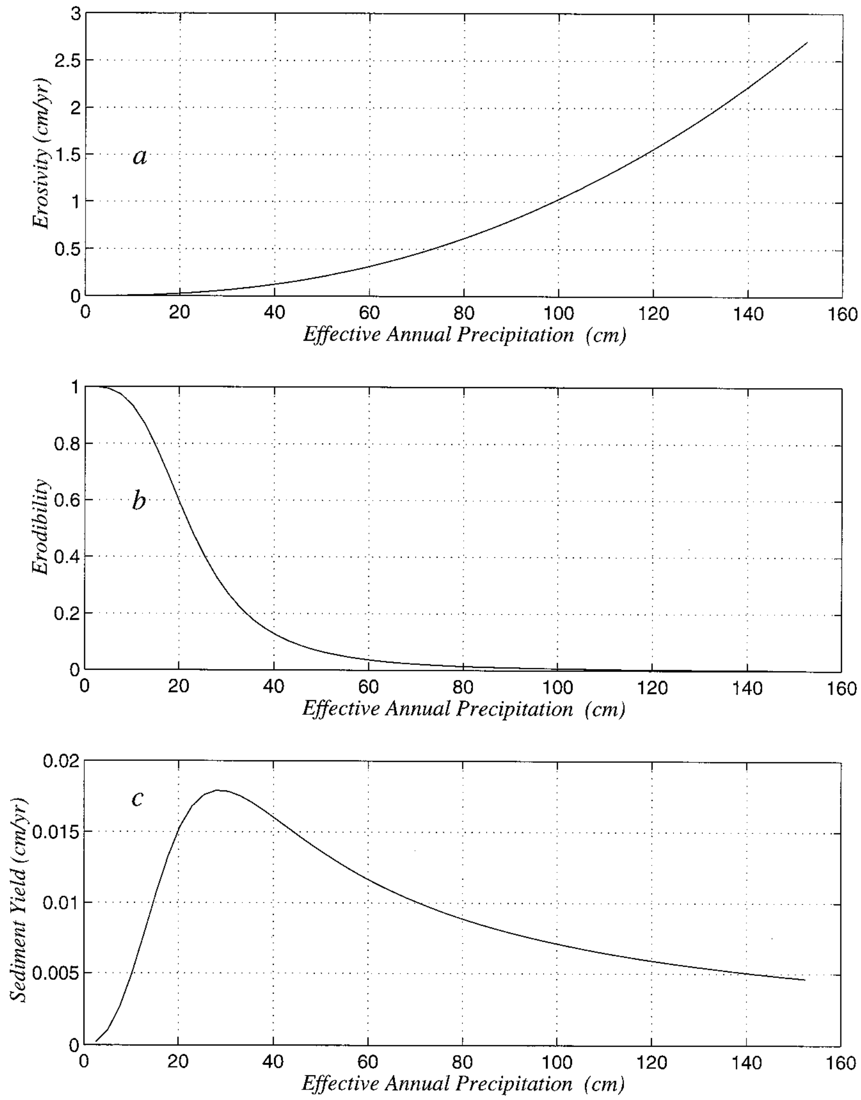

Figure 1. (a) Erosivity, (b) erodibility, and (c) sediment yield as a function of climate. From (2), $a = 2.58 \times 10^{-5}$, $b = 3.14 \times 10^{-5}$, $\alpha = 2.3$, and $\beta = 3.33$. After *Langbein and Schumm* [1958].

Drainage density is not a simple function of precipitation. It is an expression of the interrelationship of climate, soil geology, and vegetation.

Langbein and Schumm [1958], building upon the earlier work of *Langbein* [1949], examined the relationship between sediment yield and mean annual precipitation across a variety of climates within the United States. Their work consisted of collecting sediment load data from 170 U.S. Geological Survey (USGS) gaging stations as well as sediment loads trapped by reservoirs. They proposed an analytical model describing their results:

$$P = \frac{aR^{\alpha}}{1 + bR^{\gamma}} \tag{2}$$

where P is the rate of sediment yield in units of volume per unit area and R is effective annual precipitation measured as a depth. The coefficients, a and b, vary depending on the units of P and R. Exponents α and γ were estimated to be 2.3 and 3.33, respectively. The numerator of (2) represents the "erosivity" of the climate and also has units of volume per unit area. Since a and α are positive, the numerator will increase as rainfall increases. This reflects the erosion producing role of water on the landscape. The denominator of (2) represents the "erodibility" of the land surface. It describes the resistance to erosion of the land surface due to both the integrity of the material itself and the vegetation growing upon it. The denominator is a decreasing function of mean annual precipitation, which is indicative of the stabilizing role of vegetation in moist climates. As treated here, erodibility is a dimensionless quantity which serves to scale the erosivity accounting for the effects of vegetation upon sediment yield. Note that the K factor used by *Strahler* [1964] in (1) is similar in spirit to the construction of (2), although the units differ.

The ratio of erosivity to erodibility is the sediment yield rate. Figure 1 shows the sediment yield rate as a function of mean annual precipitation. The shape of this function illustrates a switch in the relative dominance of erosivity and erodibility. In arid climates, erosivity dominates and the yield rate increases as precipitation increases. As the climate grows more moist, the vegetation becomes more dense and the erodibility of the land surface reduces the yield rate as precipitation increases.

Few studies of the relationship between drainage density

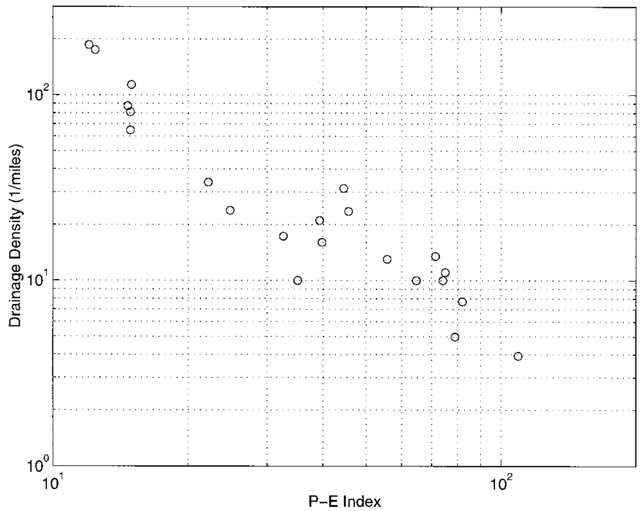

Figure 2. Observed drainage density as a function of the Thorthwaite P-E index. After *Melton* [1957].

and climate exist. Perhaps the most exhaustive study was undertaken by *Melton* [1957]. This study included 80 basins in the U.S. southwest ranging in climate from arid to humid. Figure 2 shows an inverse relationship between the Thornthwaite Precipitation Effectiveness index (or P-E index) and drainage density reported by Melton. The P-E index, I, is defined by *Thornthwaite* [1931] to be

$$I = 10 \sum_{i=1}^{12} \frac{d_i}{E_i} \tag{3}$$

where d_i and E_i are the precipitation and evaporation depths in month i. When evaporation values are not available, monthly temperatures are used instead,

$$I = 115 \sum_{i=1}^{12} \left(\frac{d_i}{T_i - 10} \right)^{1.11} \tag{4}$$

where T_i is the average monthly temperature in degrees Fahrenheit, and precipitation is measured in inches. The P-E index is a measure of climate, as indicated in Table 1.

Gregory and Gardiner [1975] and *Gregory* [1976] present similar analyses to Melton's work, showing large variability in drainage density under a dry regime and much smaller variability as the climate grows wetter. Unlike Melton, Gregory and Gardiner employ mean annual rainfall as their index of climate. Drawing a mean trend through their data (see Figure 3) is of dubious value; however, their observations suggest three regions of behavior: (1) For mean annual precipitation ≤50 cm, drainage density increases with precipitation; (2) between 50 and 100 cm, drainage density decreases with precipitation; and (3) for precipitation exceeding 100 cm annually, drainage density seems to show a slight positive trend with precipitation. Though their indices were different, it appears that Melton's data was primarily in the second regime of that described by Gregory and Gardiner, with perhaps the great variability under dry conditions accounting for Melton's failure to indicate a positive correlation between drainage density and precipitation in a desert climate.

Table 1. Climate Corresponding to Various Ranges of the Thorthwaite Precipitation-Effectiveness Index

Climatic Regime	P-E Index, I
Rainforest	≥128
Forest	64–127
Grassland	32–63
Steppe	16–31
Desert	≤15

Care should be taken when making comparisons between Figures 1, 2, and 3. In each figure the abscissa quantifies the precipitation element of climate, but in no two figures are the units directly comparable. In Figure 1 Langbein and Schumm use "effective annual precipitation." In Figure 2 Melton employs Thornthwaite's "precipitation effectiveness index." Finally, in Figure 3, Gregory and Gardiner present their results simply as a function of mean annual precipitation. The information presented in these figures should therefore be interpreted in a qualitative rather than quantitative sense.

Recently, *Rinaldo et al.* [1995] used a simple mathematical representation of landscape evolution to investigate whether a "particular landscape is in balance with current climate driven processes, or contains relict signatures of past climates" (p. 632). They study the case where annual precipitation depths change with climate. The model is forced with a sinusoidal climate fluctuation. They conclude that "wet and dry" states leave geomorphological signatures only when there is no active uplift. With active uplift the "topography tracks the current climate and any relict features are likely to reflect only the wettest condition previously experienced by the landscape" (p. 632). They show drainage density at its peak during periods where the critical shear stress for erosion is low, which they equate with wetter periods. Inversely, low drainage density occurs at high shear stress, or dry periods. In their work they acknowledge that "landscape response to (for example) varying precipitation can have significant lags and complexities associated with vegetation response" (p. 633).

In the following we will explore the relationship between drainage density and climate trying to account for the sometimes counterbalancing effects of precipitation and vegetation.

3. Theory

Fundamental to the analysis presented here is the assumption of a landscape in equilibrium with its surroundings. The landscape is subjected to various weathering agents, principally water, wind, gravity, land use, and temperature variation. The landscape maintains an equilibrium state by eroding at each point the same amount of material that is made available from weathering. We will consider two different forms of erosion or sediment transport: fluvial and diffusive. Here we use fluvial transport to describe the movement of sediment from a concentrated flow of water. In contrast, diffusive transport is a term we use to broadly define the numerous forms of sediment transport which tend to round and smooth the landscape.

Fluvial transport, Q_f, is often expressed as a power law function of discharge, Q, and local slope, S,

$$Q_f = \beta_1 Q^{m_1} S^n \tag{5}$$

where m_1 and n may vary somewhat. Values may range from 0 to 3 for m_1 and from 1 to 3 for n where (5) quantifies a

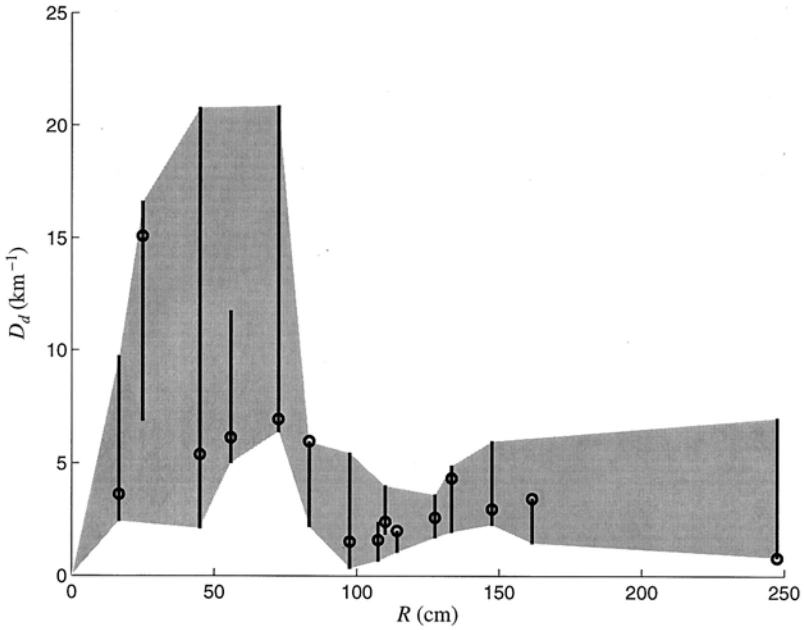

Figure 3. Observed drainage density as a function of mean annual precipitation. After *Gregory* [1976]. Copyright by John Wiley and Sons Limited. Reprinted with permission.

variety of processes including soil creep, rain splash, soil wash, and sediment transport in rivers [*Kirkby*, 1971]. The coefficient, β_1, depends upon the units of discharge and sediment transport. Discharge is often related to cumulative area, A, by a similar power law relation,

$$Q = \beta_2 A^{m_2} \tag{6}$$

where m_2 can be obtained by flood frequency analysis. Values for m_2 ranging from 0.6 to 0.8 are typical.

Diffusive transport, Q_d, is proportional to the local slope with a diffusion coefficient, D, quantifying the transport within a particular basin,

$$Q_d = DS \tag{7}$$

The total sediment transport, Q_{s_1}, at any point in space is the sum of these two erosion terms,

$$Q_{s_1} = Q_f + Q_d = \beta_1 \beta_2^{m_1} A^{m_1 m_2} S^n + DS \tag{8}$$

Equation (8) is consistent in spirit to several evolution models recently developed [e.g., *Willgoose*, 1991; *Howard*, 1994; *Tucker and Slingerland*, 1994]. Each of these models characterizes total sediment transport as the sum of fluvial and diffusive processes acting in tandem.

Let P equal the rate of sediment yield, where P is in units of length/time. The volume rate of sediment yield made available for transport in a region of area, A, is then

$$Q_{s_2} = PA \tag{9}$$

At equilibrium, the volume rate of sediment yield is balanced by the transport rate allowing the topography to remain dynamically unchanged,

$$Q_{s_1} = Q_{s_2} \tag{10}$$

or

$$PA = \beta_1 \beta_2^{m_1} A^{m_1 m_2} S^n + DS \tag{11}$$

As defined by (8), fluvial and diffusive transport are both present at all scales. A simplifying assumption can generally be made that at small scales diffusive transport is the dominant term of (11), while at large scales fluvial transport is dominant. Equation (11) can be decoupled and solved for two asymptotic relationships. For fluvial transport,

$$PA = \beta_1 \beta_2^{m_1} A^{m_1 m_2} S^n \tag{12}$$

which can be solved for the equilibrium slope as a function of cumulative area,

$$S = \left(\frac{P}{\beta_1 \beta_2^{m_1}} \right)^{1/n} A^{(1 - m_1 m_2)/n} \tag{13}$$

Similarly for diffusive transport,

$$PA = DS \tag{14}$$

which when solved for slope gives,

$$S = \frac{PA}{D} \tag{15}$$

A plot of slope versus area is shown in Figure 4 with the asymptotic equations, (13) and (15), shown as f_1 and f_2, respectively. We can calculate the critical area, A_*, at which these two asymptotes intersect by equating (13) and (15). The result gives

$$A_* = P^{(n-1)/(1-m_1 m_2 - n)} D^{-n/(1-m_1 m_2 - n)} \beta_1^{1/(1-m_1 m_2 - n)} \beta_2^{m_1/(1-m_1 m_2 - n)} \tag{16}$$

Equation (16) indicates a value for area at which both fluvial and diffusive transport yield the same local slope under conditions of dynamic equilibrium. In reality, this slope is not realized since it is precisely in this range of values of area that both diffusive and fluvial transport are of comparable magnitudes. The actual observed slope is somewhat less, as indicated by Figure 4. This critical area, A_*, quantifies the scale at which

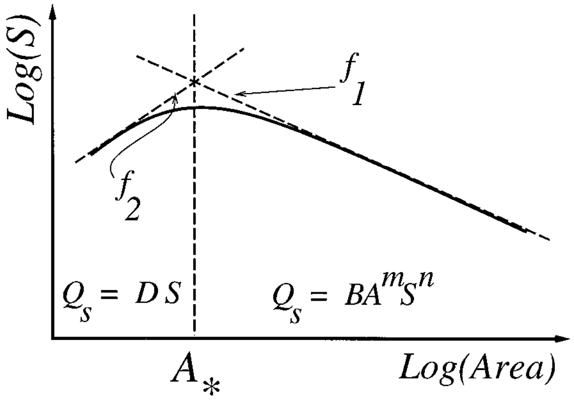

Figure 4. Theoretical slope-area relationship and the definition of the critical area, A_*. Asymptotic equations (13) and (15) are shown as f_1 and f_2, respectively.

fluvial transport becomes dominant to diffusive transport. The critical area is interpreted as a representative scale at which channelization may begin to be observed in the topography. A large value for A_* is indicative of a smooth, relatively featureless topography, while a small A_* would indicate a rugged topography dissected by channels to a great degree.

Horton [1945] defined drainage density, D_d, as the sum of the lengths of all streams in a basin of divided by the basin area, A,

$$D_d = \frac{\sum L_i}{A} \tag{17}$$

where L_i is the length of a single stream within the basin. There is a relationship between the critical area given by (16) and drainage density. Table 2 shows seven digital elevation model (DEM) data sets from throughout the United States. Channel source area was allowed to vary over several orders of magnitude. For each assumed source area the resulting drainage density was determined. All data sets exhibited a power law decline in drainage density with increasing source area of the form

$$D_d = cA_*^{-\eta} \tag{18}$$

where η was found to be very stable, ranging from about 0.45 to 0.57. Table 2 details the observed variation in η and the range over which (18) was found to be applicable. These results are consistent with the results presented by *Rodriguez-Iturbe et al.* [1992].

Combining (16) with (18) gives an equation for drainage density as a function of the sediment yield rate P and the various parameters associated with fluvial and diffusive transport.

$$D_d = c\left(P^{(n-1)/(1-m_1m_2-n)} D^{-n/(1-m_1m_2-n)} \beta_1^{1/(1-m_1m_2-n)} \beta_2^{m_1/(1-m_1m_2-n)}\right)^{-\eta} \tag{19}$$

Table 2. DEM Inferred Relationship Between Source Area and Drainage Density

Basin	State	η	Source Area Range of Applicability, km^2	R^2 (n)
Binghamton	New York	0.51	0.1–300	0.998 (30)
Brushy	Alabama	0.45	0.01–30	0.998 (29)
Buck	California	0.46	0.01–30	0.996 (29)
Calder	Idaho	0.45	0.02–20	0.999 (27)
Kaaterskill	New York	0.57	0.01–1	0.994 (18)
North Elk	Idaho	0.48	0.1–30	0.986 (22)
Racoon	Pennsylvania	0.47	0.01–40	0.999 (30)

Our objective is to characterize the variation in drainage density associated with a changing climate. While a reasonable argument can be made that many of the parameters appearing in (19) might be expected to vary with climate, this paper will exclusively examine the variation of drainage density as only the sediment yield rate, P, varies with climate. As our results will show, this sediment yield rate, as governed by the interaction between vegetation and rainfall, appears to be the essential ingredient in describing the variation of drainage density with climate. Under this scenario, two terms in (19) become a function of climate. The analysis of *Langbein and Schumm* [1958], presented earlier, expresses the sediment yield, P, as a function of effective annual rainfall, R. Their analysis quantified an integrated view of the competition between rainfall and vegetation in controlling the resulting sediment yield.

Equation (6) quantifies the discharge associated with a single precipitation depth: the 100-year storm, for example. As the climate becomes wetter or drier, the magnitude of the 100-year storm will vary. This equation must be modified to reflect this change. The exponent, m_2, in (6) will remain stable, but β_2 becomes a function of R such that

$$\beta_2 = \beta_2(R) = \xi R \tag{20}$$

where we have assumed a linear dependence between rainfall depth and discharge. We performed a small analysis using data from *Dalrymple* [1964] and *McCuen* [1989] and confirmed that this assumption is satisfactory and consistent with the assumptions and spirit of parameterizations presented elsewhere in this paper.

By combining the relationship given earlier from Langbein and Schumm with (19) and (20) we get

$$D_d = c\left[\left(\frac{aR^\alpha}{1+bR^\gamma}\right)^{(n-1)/(1-m_1m_2-n)} D^{-n/(1-m_1m_2-n)} \beta_1^{1/(1-m_1m_2-n)} \cdot (\xi R)^{m_1/(1-m_1m_2-n)}\right]^{-\eta} \tag{21}$$

Equation (21) can now be studied for the sensitivity of drainage density to changes in effective annual rainfall.

4. Discussion

The ramifications of the function described by (21) merit further study. In particular, the fact that (21) exhibits a maximum for some intermediate value of effective annual precipitation (see Figure 5a) is crucial to the existence of two distinct regimes of topographic evolution that will follow from variation in climate. In desert to semidesert conditions, with effective annual precipitation less than about 25 cm, the drainage density increases with precipitation. However, in relatively humid conditions, with effective annual precipitation exceeding 25 cm, the drainage density decreases with precipitation. The prediction that drainage density should decrease with increasing precipitation in the latter climatic regime is consistent with field observations [*Melton*, 1957; *Gregory and Gardiner*, 1975],

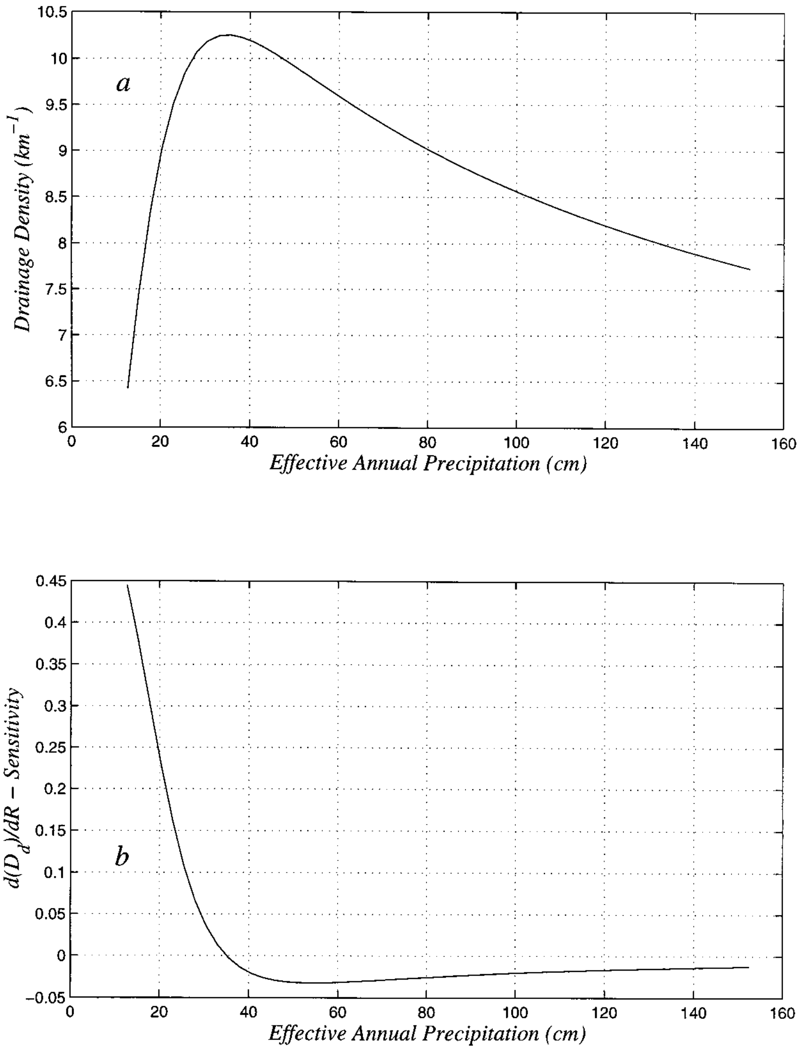

Figure 5. (a) Drainage density and (b) sensitivity of drainage density to effective annual precipitation as a function of effective annual precipitation.

as illustrated in Figures 2 and 3. Also included in Figure 5b is the sensitivity of drainage density to precipitation. The sensitivity of drainage density in desert regions is significantly larger than the same variable under relatively humid conditions, consistent with the large range of variability documented by Gregory and Gardiner and shown in Figure 3. A badland topography studied by *Howard* [1997] exhibited increased drainage density in regions of higher relief. By noting that sediment yield increases with increasing relief, we find that (21) is also consistent with Howard's observation.

The relationship between drainage density and climate is illustrated by studying the variability in drainage density that may result from sinusoidal variability in precipitation. Figure 6 shows the results for three different regimes: desert conditions with effective annual precipitation less than 20 cm, humid conditions with annual precipitation exceeding 50 cm, and intermediate conditions between these two extremes. For desert conditions vegetation is sparse, and the drainage density is directly in phase with precipitation variability; relatively wet (dry) climate corresponds to high (low) drainage density. Under humid conditions, variability in drainage density is dominated by the reduced erodibility caused by enhanced growth of vegetation. Drainage density is 180° out of phase with precipitation variability: relatively wet (dry) conditions correspond to low (high) drainage density. In between these two cases, maximum drainage density occurs at an intermediate annual precipitation depth with lower drainage densities produced by changes to either drier or wetter climates. It is interesting to note that although this response of drainage density is insensitive to the direction of the change in climate, the processes leading to this response are quite different. As climate gets drier, drainage density decreases because of the dominance of the role of precipitation in dictating erosivity; while as climate gets wetter, drainage density decreases because of the dominance of the role of vegetation in reducing the erodibility of the land surface.

5. Conclusions

The sign of the response of drainage density to any climate change depends not only on the direction of the change in climate but also on the prevailing climatic regime. This dependency on present climate is associated with the presence and degree of vegetation corresponding to this climate. Without

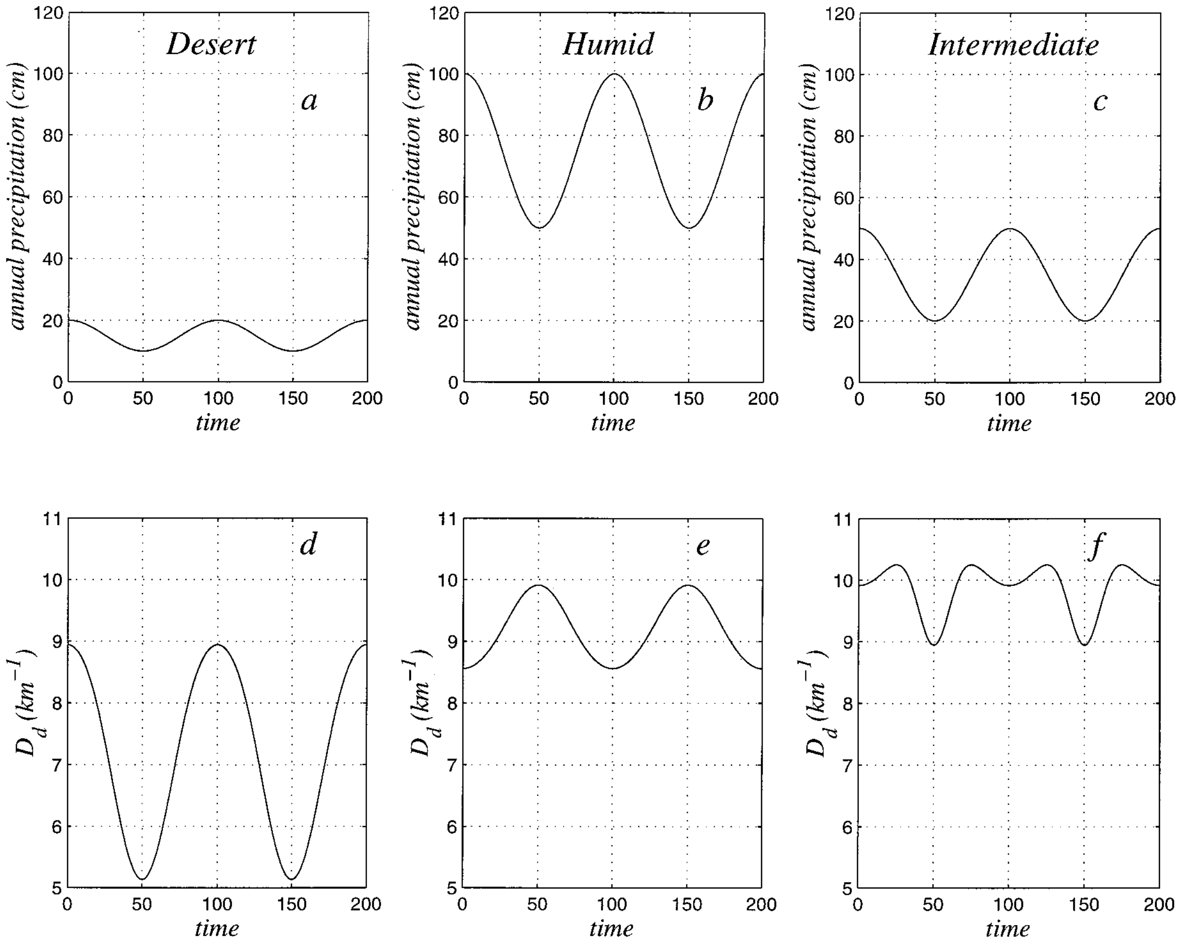

Figure 6. Variation in drainage density from a sinusoidally varying climate. Each pair of plots illustrates the time evolution of precipitation and drainage density for (a, d) desert conditions, (b, e) humid conditions, and (c, f) intermediate conditions.

vegetation, drainage density is simply related to annual precipitation. The wetter the climate, the greater the degree to which the topography will be dissected by the drainage network. With vegetation a balance between the erosive forces of precipitation and the stabilizing forces of vegetative growth must be achieved. Analytical derivations presented here are consistent with field observations from previous studies, showing theoretically that vegetation actually outstrips precipitation in humid climates to the extent that there is an observed decline in drainage density as the climate grows wetter. Some elements of the research presented here are qualitative in nature; however, this work presents a strong theoretical basis for the field observed existence of the two distinct regimes of behavior in drainage density.

Further study in this area should address the simplified parameterization scheme used here to quantify fluvial and diffusive erosion. In particular, any dependency of the fluvial and diffusive erosion parameterization on changing precipitation depths associated with climate change would add insight to the investigation presented here. Additional research examining the temporal response of the topography to climate change would elucidate which timescales are most critical to landscape evolution.

Notation

- a coefficient quantifying the change in erosivity with effective annual rainfall.
- b coefficient quantifying the change in erodibility with effective annual rainfall.
- c coefficient quantifying the change in drainage density with source area.
- d_i precipitation depth in month i.
- g acceleration due to gravity.
- m_1 exponent on discharge in fluvial transport equation.
- m_2 exponent on drainage area as a surrogate for discharge.
- n exponent on slope in fluvial transport equation.
- A drainage basin area.
- A_* source area draining to the head of a channel.
- D diffusion coefficient in diffusive transport equation.
- D_d drainage density.
- E_i evaporation depth in month i.
- H total relief of drainage basin.
- I Thornthwaite's precipitation effectiveness index.
- K Strahler's erosion proportionality factor.
- L_i length of a single stream or reach within the drainage basin.

P rate of sediment yield.
Q channel discharge.
Q_d diffusive sediment transport.
Q_f fluvial sediment transport.
Q_r Strahler's runoff intensity.
Q_{s_1} total sediment transport.
Q_{s_2} volume rate of sediment production.
R effective annual rainfall.
S local topographic slope.
T_i average monthly temperature.
α exponent quantifying the change in erosivity with effective annual rainfall.
β_1 coefficient quantifying the change in fluvial sediment transport with discharge.
β_2 coefficient quantifying the change in discharge with drainage basin area.
γ exponent quantifying the change in erodibility with effective annual rainfall.
η exponent quantifying the change in drainage density with channel source area.
μ dynamic viscosity of the fluid.
ξ coefficient quantifying the change in discharge with effective annual rainfall.
ρ density of the fluid.

Acknowledgments. We would like to thank Garry Willgoose and Daniele Veneziano and the comments from two anonymous reviewers for their valuable input to earlier drafts of this manuscript. This work was supported by the U.S. Army Research Office (DAAH04-95-1-0181).

References

Dalrymple, T., Flood characteristics and flow determination, in *Handbook of Applied Hydrology*, edited by V. T. Chow, pp. 25.5–25.7, McGraw-Hill, New York, 1964.

Gregory, K. J., Drainage networks and climate, in *Geomorphology and Climate*, edited by E. Derbyshire, pp. 289–315, John Wiley, New York, 1976.

Gregory, K. J., and V. Gardiner, Drainage density and climate, *Z. Geomorphol. N.F.*, *19*, 287–298, 1975.

Gregory, K. J., and D. E. Walling, The variation of drainage density within a catchment, *Int. Assoc. Sci. Hydrol. Bull.*, *13*, 61–68, 1968.

Horton, R. E., Erosional development of streams and their drainage basins: Hydrophysical approach to quantitative geomorphology, *Bull. Geol. Soc. Am.*, *56*, 275–370, 1945.

Howard, A. D., A detachment-limited model of drainage basin evolution, *Water Resour. Res.*, *30*, 2261–2285, 1994.

Howard, A. D., Badland morphology and evolution: Interpretation using a simulation model, *Earth Surf. Processes Landforms*, *22*(3), 211–227, 1997.

Kirkby, M. J., Hillslope process-response models based on the continuity equation, in *Slopes: Form and Process*, *Spec. Publ. 3*, pp. 15–30, Inst. of Br. Geogr., London, 1971.

Langbein, W. B., Annual runoff in the United States, *U.S. Geol. Soc. Circ. 52*, 11 pp., 1949.

Langbein, W. B., and S. A. Schumm, Yield of sediment in relation to mean annual precipitation, *Eos Trans. AGU*, *39*(6), 1076–1084, 1958.

McCuen, R. H., *Hydrologic Analysis and Design*, pp. 138–140, Prentice-Hall, Englewood Cliffs, N. J., 1989.

Melton, M. A., An analysis of the relations among elements of climate, surface properties, and geomorphology, *Dept. Geol. Columbia Univ. Tech. Rep. 11*, *Proj. NR 389-042*, Off. of Nav. Res., New York, 1957.

Montgomery, D. R., and W. E. Dietrich, Where do channels begin?, *Nature*, *336*, 232–234, 1988.

Montgomery, D. R., and W. E. Dietrich, Landscape dissection and drainage area-slope thresholds, in *Process Models and Theoretical Geomorphology*, edited by M. J. Kirkby, pp. 221–246, John Wiley, New York, 1994.

Montgomery, D. R., and E. Foufoula-Georgiou, Channel network source representation using digital elevation models, *Water Resour. Res.*, *29*(12), 3925–3934, 1993.

Rinaldo, A., W. E. Dietrich, R. Rigon, G. K. Vogel, and I. Rodriguez-Iturbe, Geomorphological signatures of varying climate, *Nature*, *374*, 632–635, 1995.

Rodriguez-Iturbe, I., E. J. Ijjasz-Vasquez, R. L. Bras, and D. G. Tarboton, Power law distributions of mass and energy in river basins, *Water Resour. Res.*, *28*(4), 1089–1093, 1992.

Schumm, S. A., Evolution of drainage systems and slopes in badlands at Perth Amboy, New Jersey, *Geol. Soc. Am. Bull.*, *67*, 597–646, 1956.

Smith, T. R., and F. P. Bretherton, Stability and the conservation of mass in drainage basin evolution, *Water Resour. Res.*, *8*(6), 1506–1529, 1972.

Strahler, A. N., Quantitative geomorphology of drainage basins and channel networks, in *Handbook of Applied Hydrology*, edited by V. T. Chow, pp. 4.39–4.76, McGraw-Hill, New York, 1964.

Thornthwaite, C. W., The climates of North America according to a new classification, *Geogr. Rev.*, *21*, 633–655, 1931.

Tucker, G. E., and R. L. Slingerland, Erosional dynamics, flexural isostasy, and long-lived escarpments: A numerical modeling study, *J. Geophys. Res.*, *99*(B6), 12,229–12,243, 1994.

Willgoose, G. R., R. L. Bras, and I. Rodriguez-Iturbe, A coupled channel network growth and hillslope evolution model, 1, Theory, *Water Resour. Res.*, *27*(7), 1671–1684, 1991.

R. L. Bras and E. A. B. Eltahir, Ralph M. Parsons Laboratory, Department of Civil and Environmental Engineering, Massachusetts Institute of Technology, Cambridge, MA 02139.

G. E. Moglen, Department of Civil Engineering, University of Maryland, College Park, MD 20742. (e-mail: moglen@eng.umd.edu)

(Received April 7, 1997; revised September 22, 1997;
accepted September 24, 1997.)